International Research Journal of Innovations in Engineering and Technology (IRJIET)

ISSN (online): 2581-3048

Volume 5, Issue 4, pp 87-96, April-2021

https://doi.org/10.47001/IRJIET/2021.504014

Analysis of the Aerodynamics Parameters and Design of the Fixed Wing for the Drone

[1]Manuel Alejandro Lira Martinez, [2]Arturo Paz Perez, [3]Christian Aguirre Terrazas, [4]Abril Abigail Solis Salazar, [5]Julio Cesar Cuellar Mata

[1,2,3,4,5]Universidad Autónoma de Ciudad Juárez. Ave. Del Charro 450 N Cd. Juárez, Chih. CP 32310, México

***Abstract* - The capacity of a wing to generate lift force is determined by the lift and drag coefficients produced by the effects of the airflow path along the selected airfoil and surface geometry. On this research, a methodology has been developed, based on the System Life Cycle management tool and mathematical models to perform a theoretical, computational, and experimental aerodynamic analysis in order to design and model a fixed wing for an UAV.**

Keywords: Aerodynamic analysis, design and model, fixed wing, Unmanned Aerial Vehicle.

I. INTRODUCTION

Designing a wing layout is an engineering process that integrates objectives, synthesis, analysis, test, evaluation, construction, and operation as fundamental elements that are continuously iterated until the accomplishment of design requirements. A management tool that "[…] includes design, development, production, operation, support, and disposal" [1], is the System Life Cycle. The application of this procedure into the methodology developed on this research, divided the wing design into two major phases, acquisition and utilization.

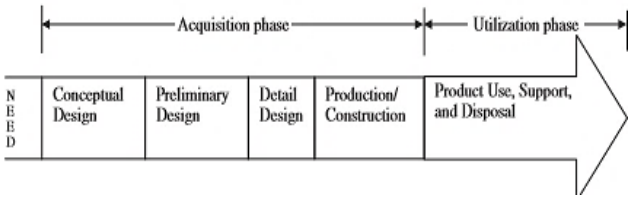

Figure 1: The system life cycle [1]

As it is illustrated on Fig. 1, in the acquisition phase, the conceptual design, preliminary design, and detailed design were performed and evaluated before constructing the fixed wing prototype.

As a basis to set the aerodynamic limitations and design purposes were taken requirements listed below:

- Design a fixed wing capable of generating a force of 245.166 N to lift the maximum gross weight of the UAV.
- Design a fixed wing capable to generate lift required with a minimum speed of 12 m/s.

In the preliminary design, the mathematical models from Sadraey and Raymer were implemented to analyze and define the optimum wing configuration, concluding that it consists on a high double taper wing using an airfoil E423. Also, a wing surface of 1.7778 m^2 was calculated with a wing loading of 137.9 $\frac{N}{m^2}$. After the theoretical analysis, a wind tunnel test was carried out to ensure that the preliminary wing layout met the objectives previously established.

During the detailed design, methods from Sadraey, Abbot, and Anderson were executed to analyze the lift distribution and performance curves to determine the optimal angle of incidence for cruise flight. Results were corroborated and evaluated with Computational Fluid Dynamics (CFD).

To end with the acquisition phase, the wing prototype was constructed using 20 ribs and 2 main spars. Each rib was located according to each section analyzed on the lift distribution curve. Finally, the prototype was used on a UAV of 22 kilograms of gross weight and propelled by a Scorpion SII-4020 electrical motor, having a successful flight circuit.

The methodology presented on this paper pretends to provide the basis to analyze and design fixed wings for UAVs with similar cargo applications. The method is briefly described in this paper throughout the Section II according with each phase of the System Life Cycle.

II.METHODS, ANALYSIS AND TESTS

In this work, the System Life Cycle was adapted for designing a wing as it is shown on Fig. 2. CDR, PDR and FDR refer to the revisions after each design stage. [1]

International Research Journal of Innovations in Engineering and Technology (IRJIET)

ISSN (online): 2581-3048

Volume 5, Issue 4, pp 87-96, April-2021

https://doi.org/10.47001/IRJIET/2021.504014

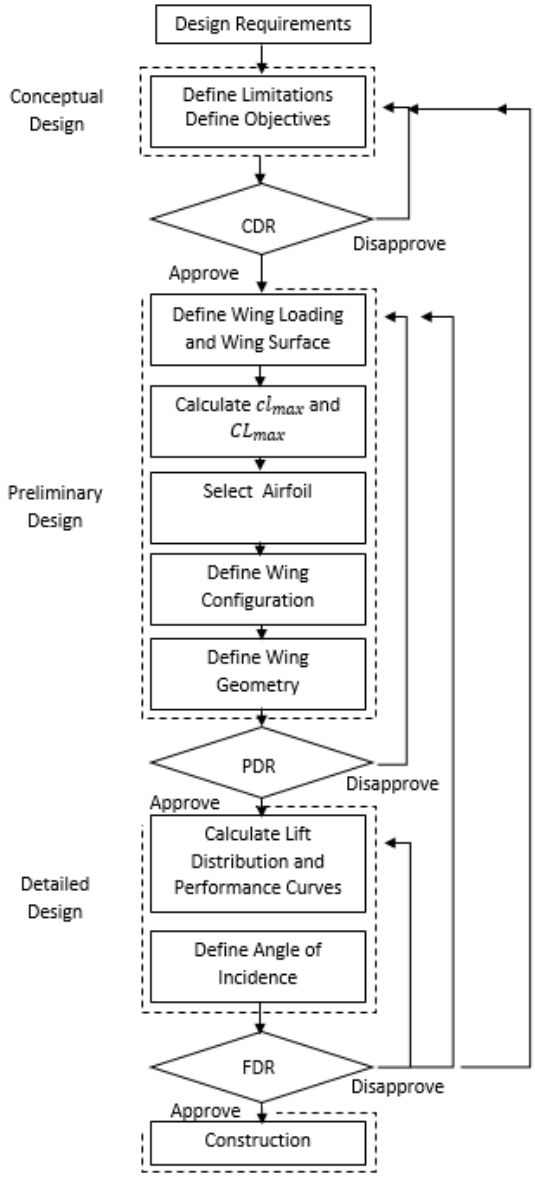

Figure 2: System Life Cycle for Designing a Wing

2.1 Design Requirements

As no restrictions or requirements were set by a customer or industry, the SAE Aero Design México 2019 rules, summarized on Table I, were considered as the UAV specifications to be accomplished. [2]

Table 1: UAV Specifications

Maximum Gross Weight	22 Kilograms
UAV configuration	Fixed Wing
Usage of FRP	FRP motor mount, propeller, landing gear and control linkage components. Rest of parts should not contain this type of material.
Propulsion System	Single electric motor
Maximum Take-Off distance	61 m
Power Limiter	2018 VI/V2 version 1000-watt power limiter.
Inner Payload	Consists of an enclosed bay inside the fuselage.
Hard Points	Consists of two external payload bays that have just one contact point with the wing.

2.2 Conceptual Design

In order to define the aerodynamic design requirements, a decision matrix was implemented to analyze which UAV specifications impacted on the wing design, and consequently, to the aerodynamic performance.

Being the gross weight, UAV configuration, and propulsion system, the specifications that affected and limited the wing design and performance [3], it was established that the wing layout should consist on a fixed wing capable to generate a force of 245.166 N to lift 22 kilograms with a minimum speed of 12 m/s [4].

2.3 Preliminary Design

2.3.1 Definition of Wing Loading and Surface

The importance to set or calculate this parameter remains of the fact that it affects the maximum lift coefficient, wing span, as well as, the take-off and landing distances. As wing loading is increased, the wing span is reduced, and vice versa [5].

A wing loading of 137.9 $\frac{\mathrm{N}}{\mathrm{m}^2}$ was selected from a database of aircrafts with similar cargo applications that has participated on previous SAE Aero Design [6] competitions. Considering this value and that the lift force equals to weight in level flight [5], it was calculated the wing surface by solving the following equation:

$$Wing\ Loading = \frac{W}{S}$$

$$\therefore$$

$$S = \frac{(245.166\ \mathrm{N})}{(137.9 \frac{N}{m^2})}$$

$$S = 1.7778\ m^2$$

2.3.2 Calculation of cl_{max} and CL_{max}

Per equation (2), it is stated that "[…] the aircraft is at maximum lift coefficient" [5] when lift equals to weight in level flight and considering the stall speed. Therefore, the CL_{max} is given by:

$$W = L = q_{stall}\, SCL_{max} = \frac{1}{2}\rho {V_{stall}}^2 SCL_{max} \quad (2)$$

International Research Journal of Innovations in Engineering and Technology (IRJIET)

ISSN (online): 2581-3048

Volume 5, Issue 4, pp 87-96, April-2021

https://doi.org/10.47001/IRJIET/2021.504014

$$\therefore$$

$$CL_{max} = \frac{2W}{\rho V_{stall}{}^2 S}$$

$$\therefore$$

$$CL_{max} = \frac{2(245.166\ \text{N})}{(1.1405\ \frac{kg}{m^3})(12\frac{m}{s})^2 (1.7778 m^2)} = 1.6793$$

The density (ρ) of 1.1405 $\frac{kg}{m^3}$ was determined by studying the environment considerations of Monterrey, the place where aircraft must operate.

Equation (3) solves the aircraft CL_{max} by considering the contributions of the fuselage, wing, tail, and other components.

$$CL_{\max w} = \frac{CL_{max}}{0.95} \quad (3)$$

$$\therefore$$

$$CL_{\max w} = \frac{1.6793}{0.95} = 1.7677$$

Finally, the cl_{max} was calculated using equation (4) and the $CL_{\max w}$, previously obtained.

$$cl_{\max gross} = \frac{CL_{\max w}}{0.90} = \frac{1.7677}{0.90} = 1.9641 \quad (4)$$

2.3.3 Selection of the airfoil

Five airfoils with approximate values to the $cl_{\max gross}$ obtained were selected to study their aerodynamic properties (cl_{max}, $\alpha_s, cd_{min}, \alpha_{cd_{min}}, cl_{\alpha=0}, \alpha_{cl=0}, cd_{cl_{max}}$) by implementing XFLR5.

Before started the Batch foil analysis on the XFLR5, the Reynolds number was calculated in order to set the flow regime at which the wing be operating.

$$Re = \frac{\rho V C}{\mu} \quad (5)$$

$$\therefore$$

$$Re = \frac{(1.1405\ \frac{kg}{m^3})(12\frac{m}{s})(0.6mts)}{1.88431 - 05} = 653{,}680.62$$

Where ρ is the density, V is the velocity at critical conditions, and C is the Mean Geometric Chord (CMG). In this case, the CMG was approximately estimated, due to there wasn't any geometry defined.

To perform the Batch Analysis following parameters were defined as follow:

- Analysis type: 1
- Range was selected
- Batch Variables
  Reynolds started at 100,000 and finished on 700,000 with increments of 1,000
  NCrit was defined as 9.00
- Analysis Range
- Alpha was selected
  Analysis started at -20 degrees and finished at +20, with increments of 1 degree.
  500 iterations were defined to perform the analysis.

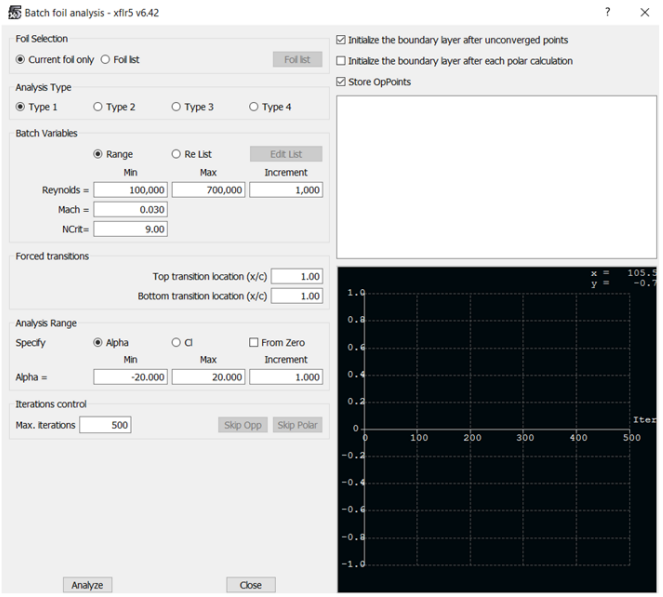

Figure 3: Batch Foil Analysis Definition

After analyzing the aerodynamic properties of each airfoil, it was selected the E423 due to the relation between its cl_{max}, angle of stall, and lift-to-drag ratio. The maximum lift coefficient obtained was 2.0536 with an angle of stall of 12 degrees and a lift-to-drag-ratio of 138.18.

2.3.4 Definition of the Wing Configuration

A high double tapered wing configuration selection was based on the study of the advantages and disadvantages of the parameters shown on tables II and III.

Table II: Advantages and Disadvantages of the Different Wing Vertical Locations [1]

Wing Vertical Location	Advantages	Disadvantages
High	-Eases loading and unloading of loads into and out of the aircraft -Makes aircraft laterally stable	-Is about 20% structurally heavier than the lower wing -Lateral control is weaker
Mid	-Has less interference drag	-Aircraft structure is heavier - Is more expensive
Low	-The wing has less induced drag -Aircraft structure is lighter	-The wing generates less lift -Aircraft has a lower landing performance

International Research Journal of Innovations in Engineering and Technology (IRJIET)
ISSN (online): 2581-3048
Volume 5, Issue 4, pp 87-96, April-2021
https://doi.org/10.47001/IRJIET/2021.504014

Table III. Advantages and Disadvantages of the Wing Types [1,7]

Wing Type	Advantages	Disadvantages
Rectangular	-Ease to manufacture -Cost	-The spanwise lift distribution is far from the elliptical -Structure is heavier
Tapered	-Reduce the wing weight -Reduce the induced drag	-Cost of manufacture increase
Double tapered	-The spanwise lift distribution is nearly elliptic. -Structure is lighter than the rectangular wing	-Cost of manufacture increased.
Elliptical	-The spanwise lift distribution is ideally elliptic. -Generates the minimum induced drag.	-Complexity of manufacture -Cost of manufacture increased

2.3.5 Definition of the Wing Geometry

Before starting sizing the wing layout, the taper ratio and aspect ratio of the wing were established.

As the aspect ratio (AR) increases, "[…] the aerodynamic features of three-dimensional wing […] are getting closer to its two-dimensional airfoil section" [1], which means that the lift-to-drag ratio also increases and provides a major aerodynamic performance. Therefore, a longer aspect ratio was desired. Taking into consideration that the aspect ratio is directly proportional with the wing span amount, and that the wing spar shouldn't exceed of 3.75 meters, due to its mechanical behavior, this value was used on equation (6) to calculate the highest AR.

$$AR = \frac{b^2}{S} = AR = \frac{(3.75\ mts)^2}{1.7778\ m^2} = 7.9098 \quad (6)$$

According with Sadraey [1] and Raymer [5], the aspect ratio range for low subsonic and home-built aircrafts is from 4 to 9. Since value obtained was inside the range it was taken as valid to continue with the geometry definition.

Due to the configuration selected, two different taper ratios were defined. Combining the advantages of the rectangular and tapered wing configurations, it was decided that a portion of the wing must consist on a rectangular surface (taper ratio of 1) and the rest must be tapered. On Fig. 5 below presented the effect of the taper ratio on lift distribution among the wingspan, and as it could be observed the nearly elliptical lift distribution is generated with values of the taper ratio between 0.8 and 0.

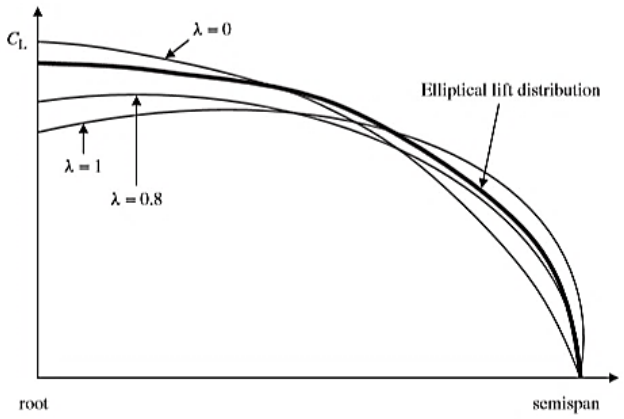

Figure 4: Effect of taper on lift distribution [1]

Consequently, taper ratios of 0.8 and 0.6 were selected to calculate different geometries and analyze the lift curves and lift-to-drag ratio on XFLR5. First, it was consider that the rectangular section would be at 25% of the half of the wing span. Then, it was iterated at 50%, 75% and 90%.

Geometrically, the total surface is integrated by the sum of the rectangular and tapered surfaces, just as expressed on equation (7).

$$S_T = S_R + S_{TR} \quad (7)$$

$$\therefore$$

$$S_T = b_R * Cr + \frac{Cr + Ct}{2} * b_{TR}$$

Where S_T is the total surface, S_R is the rectangular surface, S_{TR} is the tapered surface, b_R is the rectangular portion of the half of the wingspan, b_{TR} is the tapered portion of the half of the wing span, Cr is the root chord, and Ct is the tip chord.

Solving the equation (8) and substituting the value of Ct into the equation (7), a function to calculate Cr was given.

$$\lambda = \frac{Ct}{Cr} \quad (8)$$

$$\therefore$$

$$Cr * \lambda = Ct$$

$$\therefore$$

$$S_T = b_R * Cr + \frac{Cr + (Cr * \lambda)}{2} * b_{TR}$$

$$\therefore$$

$$S_T = Cr\left[b_R + \left(\frac{1+\lambda}{2} * b_{TR}\right)\right]$$

$$\therefore$$

$$Cr = \frac{S_T}{\left[b_R + \left(\frac{1+\lambda}{2} * b_{TR}\right)\right]}$$

By varying the taper ratio and the rectangular sections along the wingspan, eight geometries were obtained and summed up on Table IV.

International Research Journal of Innovations in Engineering and Technology (IRJIET)

ISSN (online): 2581-3048

Volume 5, Issue 4, pp 87-96, April-2021

https://doi.org/10.47001/IRJIET/2021.504014

Table IV: Wing Geometries

%b/2	Λ	b_R	b_{TR}	Cr	Ct
0.25	0.8	0.4687	1.4062	0.5125	0.4100
0.50	0.8	0.9375	0.9375	0.4990	0.3992
0.75	0.8	1.4062	0.4687	0.4862	0.3890
0.90	0.8	1.6875	0.1875	0.4788	0.3831
0.25	0.6	0.4687	1.4062	0.5577	0.3346
0.50	0.6	0.9375	0.9375	0.5267	0.3160
0.75	0.6	1.4062	0.4687	0.4990	0.2994
0.90	0.6	1.6875	0.1875	0.4837	0.2902

The geometries were defined on XFLR5 and analyzed under the following conditions:

- Analysis type 1
- Free stream speed: 12 m/s
- Analysis: LLT
- Aero Data
  - Density: 1.1405 $\frac{kg}{m^3}$
  - Viscosity:1.88e-05

On Fig. 6 and 7 are shown the lift and performance curves given by XFLR5. Analyzing the results of the lift coefficients and lift-to-drag-ratio, it was determined that when the 50% of the wing span is rectangular and the rest tapered, it provides the major aerodynamic performance.

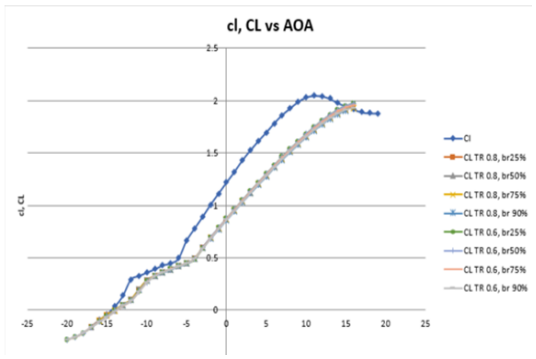

Figure 6: Lift Curves

An efficiency of 19.03 was given by the geometry selected and a maximum lift coefficient of 1.9757 at 16 degrees.

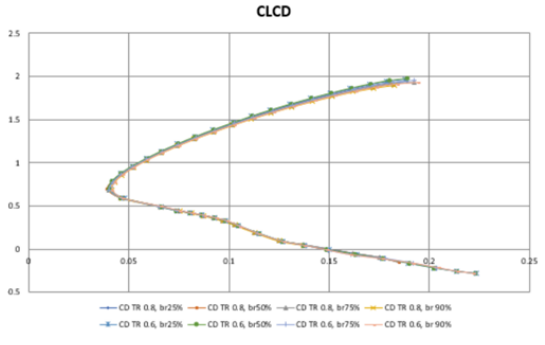

Figure 7: CLCD Curves

2.3.6 Preliminary Design Review

The wing geometry was scaled 1:15, which means that all the dimensions were reduced at the 15% of the total amount. Once scaled, a 3D print prototype was used on the wind tunnel in order to compare the lift given by XFLR5 and the experimental result of the test.

The maximum lift coefficient given by the wind tunnel test at 12 m/s was 1.9545, having a 97.4812% of approximation with the computational outcome.

2.4 Detailed Design

2.4.1 Calculation of Lift Distribution and Performance Curves

Employing the Anderson's Method [8] it was calculated the lift distribution along the wing span. This procedure consists of eight columns that are presented and explained below.

1	2	3	4
Section	Y	C	La
0	0	0.526771852	1.136263
0.2	0.375	0.526771852	1.123812
0.4	0.75	0.526771852	1.110722
0.5	0.9375	0.526771852	1.054906
0.6	1.125	0.484571852	0.99909
0.8	1.5	0.400171852	0.807459
0.9	1.6875	0.357971852	0.637098
0.95	1.78125	0.336871852	0.493737
0.975	1.828125	0.326321852	0.361918
1	1.875	0.315771852	0

Lift Distribution		
5	6	7
Lb	Clb	Cla1
0	0	1.02263689
0	0	1.01683099
0	0	0.99964999
0	0	0.94941558
0	0	0.97748833
0	0	0.9566192
0	0	0.84376696
0	0	0.69485806
0	0	0.52581041
0	0	0

8							
Cl=Clb+CL*Cla1							
CL							
0.2	0.6	1	1.5	1.9	2	2.001	2.007
0.204527378	0.613582134	1.022636889	1.533955335	1.943010091	2.045273778	2.046296416	2.052432238
0.203366198	0.610098593	1.016830999	1.525246483	1.931978879	2.033661988	2.034678808	2.040779794
0.199929997	0.599789991	0.999649999	1.499474978	1.899334972	1.999299997	2.000299621	2.006297521
0.189883115	0.569649346	0.949415558	1.424123364	1.803889595	1.898831155	1.899780568	1.905477061
0.195497665	0.586492996	0.977488333	1.466232489	1.85722782	1.954976655	1.955954141	1.961619071
0.19132384	0.57397152	0.9566192	1.434928799	1.817576479	1.9132384	1.914195018	1.919934733
0.168753391	0.506260174	0.843766696	1.265650435	1.603157218	1.687533911	1.688337768	1.693440282
0.138971612	0.416914837	0.694858061	1.042287092	1.320230316	1.389716122	1.390410981	1.394580129
0.105162081	0.315486244	0.525810405	0.788715609	0.999039771	1.051620811	1.052146622	1.055301485
0	0	0	0	0	0	0	0

Figure 9: Lift Distribution Calculation

International Research Journal of Innovations in Engineering and Technology (IRJIET)

ISSN (online): 2581-3048

Volume 5, Issue 4, pp 87-96, April-2021

https://doi.org/10.47001/IRJIET/2021.504014

Column 1: Refers to the wing section that is being studied.

Column 2: Is the product of the half of the span value and the Column 1.

Column 3: Refers to the corresponding chord size at the wing section indicated.

Column 4: Refers to the additional lift given by Abbot's [9] work.

Column 5: Refers to the basic lift given by Abbot's [8] work. (If the wing doesn't have a twist angle, do not fill this column, see details on column 6)

Column 6: Refers to the basic lift coefficient given by:

$$Clb = \frac{\epsilon a_e s}{cb} Lb = \frac{(1)(0.0862\frac{1}{\circ})(25.40m^2)}{c(15.88m)} Lb (9)$$

Where ϵ is the twist angle of the wing, a_e is the wing slope, s is the surface, c is the CMG, b the wing span and Lb the basic lift. In this case, as the twist angle is 0, the entire column has a value of 0.

Column 7: Refers to the additional lift coefficient given by:

$$Cla1 = \frac{S}{cb} La \quad (10)$$

Where, the surface is S, c is the CMG, b the wing span, and La the additional lift.

Column 8: Refers to the wing lift coefficient given by:

$$C_l = Cl_b + CL * Cla1 (11)$$

The lift distribution obtained is shown on Fig. 10. The maximum wing lift coefficient given by this distribution was 2.00.

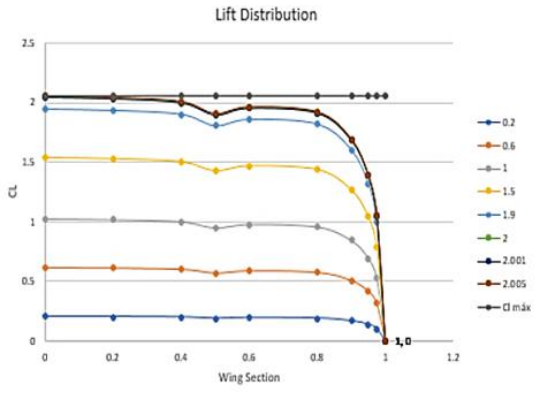

Figure 10: Lift Distribution

To calculate the wing slope, the methodology of Abbot [8] was implemented. First, the airfoil slope was calculated by taking the two points that describe the linear part of the curve as it is shown on Fig. 11.

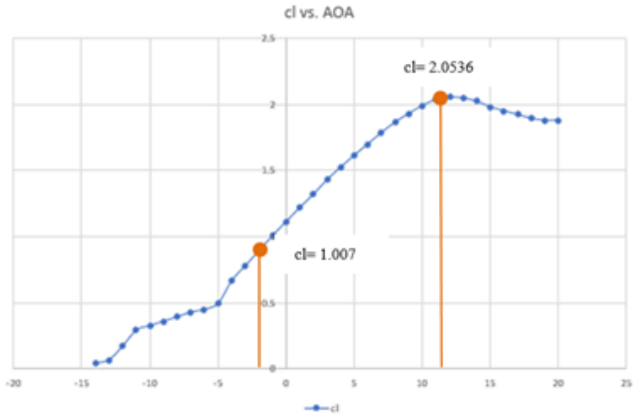

Figure 11: Airfoil Slope Curve

$$\boldsymbol{a_0} = \frac{\boldsymbol{cl_{\alpha=12} - cl_{\alpha=-1}}}{12° - (-1°)} = \frac{2.0536 - 1.007}{12° - (-1°)} = 0.0805 \frac{1}{\circ} (11)$$

After the airfoil slope calculation, the perimeter was defined by summing all the distances around the two-dimensional wing geometry.

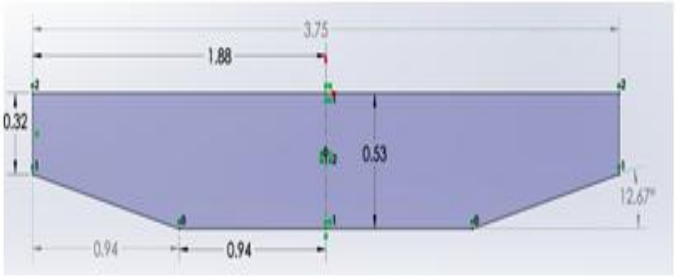

Figure 12: Wing Perimeter

Then, factor $ae$was given by solving equation (12).

$$ae = \frac{a_0}{E} \quad (12)$$

Where:

$$E = \frac{Wing\ perimeter}{2b} (13)$$

$$\therefore$$

$$E = \frac{8.1789\ m}{2(3.75m)} = 1.0905$$

$$\therefore$$

$$\boldsymbol{a_e} = \frac{0.0805\frac{1}{\circ}}{1.0905} = 0.0257\frac{1}{\circ}$$

International Research Journal of Innovations in Engineering and Technology (IRJIET)
ISSN (online): 2581-3048
Volume 5, Issue 4, pp 87-96, April-2021
https://doi.org/10.47001/IRJIET/2021.504014

Then, a factor $f = 0.9975$ was obtained from Fig. 13 by the intersection of the aspect ratio with the taper ratio.

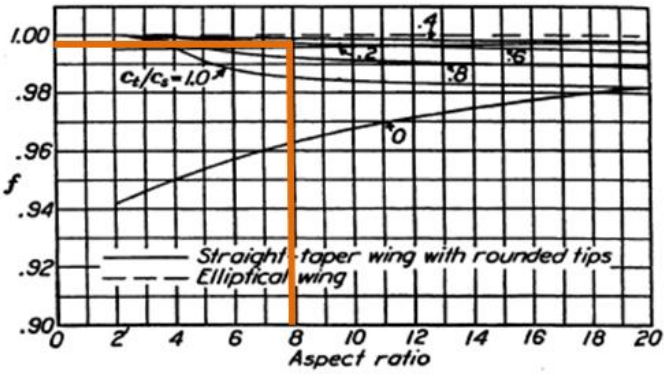

Figure 13: Chart for Determining Lift-Curve Slope [8]

Finally, the wing slope was calculated by employing equation (14).

$$\boldsymbol{a} = \frac{\boldsymbol{a_e}}{1 + \frac{57.3\boldsymbol{a_e}}{\pi AR}} (14)$$

$$\therefore$$

$$\boldsymbol{a} = \frac{0.0257\frac{1}{\circ}}{1 + \frac{57.3(0.0257\frac{1}{\circ})}{\pi(7.9098)}} = 0.0629\frac{1}{\circ}$$

Once it was obtained the wing slope, the angle of zero lift of the wing was giving by:

$$\alpha_{CL=0} = \alpha_{cl=0} + J\varepsilon \quad (15)$$

Where, the angle of attack of zero lift of the airfoil is $\alpha_{cl=0}$, J is a factor for determining the angle of attack [8], and ε is the twist angle. Factor J is given by the intersection of the aspect ratio with the taper ratio on chart shown on Fig. 14; however, this value wasn't defined due to ε=0.

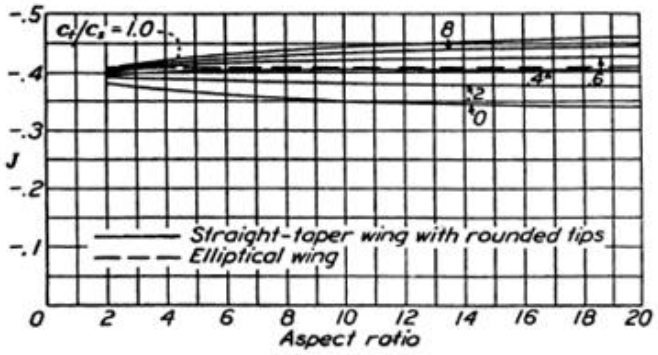

Figure 14: Chart for Determining Angle of Attack [8]

Then:

$$\alpha_{CL=0} = \alpha_{cl=0}$$
$$\therefore$$
$$\alpha_{CL=0} = -14°$$

Due to a section of the wing slope curve is linear, Abbot [8] established the following mathematical model to graph the curve.

$$CL = m\alpha + CL_{\alpha=0} \quad (16)$$

Where, $\boldsymbol{a}=m$ since it is the wing slope, α is the angle of attack, and $CL_{\alpha=0}$ is the wing lift coefficient at zero angle of attack. Solving equation (16) and substituting the value of equation (15) it was set that the value of the $CL_{\alpha=0} = 0.8810$.

$$0 = (0.0629\frac{1}{\circ})(-14°) + CL_{\alpha=0}$$
$$\therefore$$
$$CL_{\alpha=0} = 0.8810$$

Known the value of the $CL_{\alpha=0}$, it was stated the mathematical model to graph the wing slope curve of the preliminary design.

$$CL = (0.0629\frac{1}{\circ})\alpha + 0.8810$$

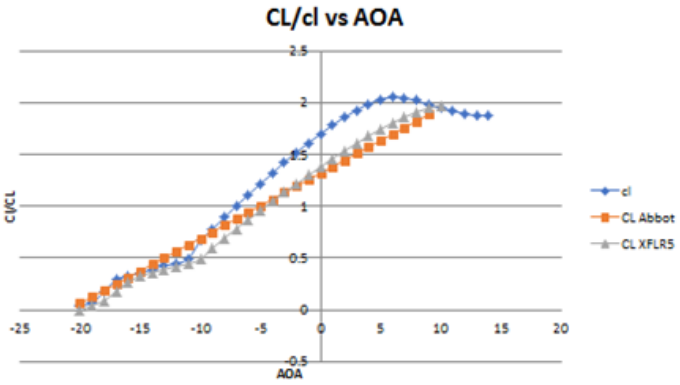

Figure 15: Wing Slope Curve

According with the analysis of the Wing Slope Curve, the maximum lift coefficient is 1.8880.

Finally, the performance curve, or drag polar, was calculated by implementing the Anderson's [9] method. First, the equation to calculate the drag coefficient was settled.

$$C_D = c_d + C_{D_i} \quad (17)$$

Where the airfoil drag coefficient is c_d, and C_{D_i} is the induced drag coefficient and is given by:

International Research Journal of Innovations in Engineering and Technology (IRJIET)

ISSN (online): 2581-3048

Volume 5, Issue 4, pp 87-96, April-2021

https://doi.org/10.47001/IRJIET/2021.504014

$$C_{D_i} = \frac{CL^2}{\pi eAR} \quad (18)$$

Where:

$$e = \frac{1}{1+\delta} \quad (19)$$

And δ=0.033 was settled by the intersection of the taper ratio with the aspect ratio on the graph shown on Fig. 16.

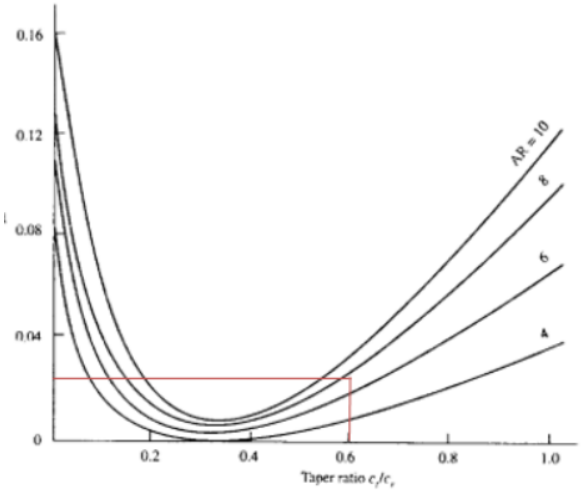

Figure 16: Induced Drag Factor as a Function of Taper Ratio for Wings of Different Aspect Ratios [9]

Then:

$$e = \frac{1}{1+0.033} = 0.9680$$

$$\therefore$$

$$C_{D_i} = \frac{CL^2}{\pi(0.9680)(7.9098)}$$

$$\therefore$$

$$C_D = 0.01056 + \frac{CL^2}{\pi(0.9680)(7.9098)}$$

Once it was calculated the lift and drag coefficients for each angle of attack, the drag polar was graphed.

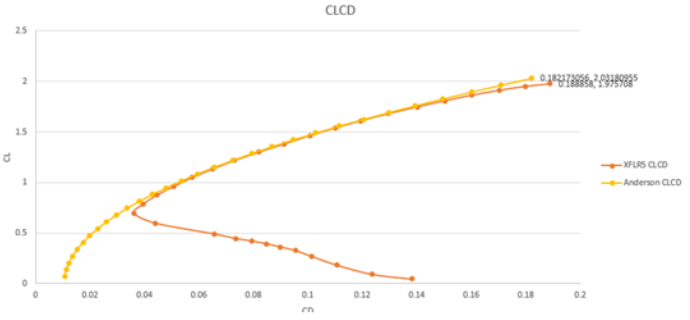

Figure 17: Drag Polar

According with the results obtained from the graph the major aerodynamic efficiency occurs at an angle of attack of 0°.

2.4.2 Final Design Review

After performed the aerodynamic analysis at the conceptual, preliminary, and detailed designs, the wing configuration was modeled on Solid Works and saved as IGS file with the purpose to evaluate the lift and drag forces on CFD.

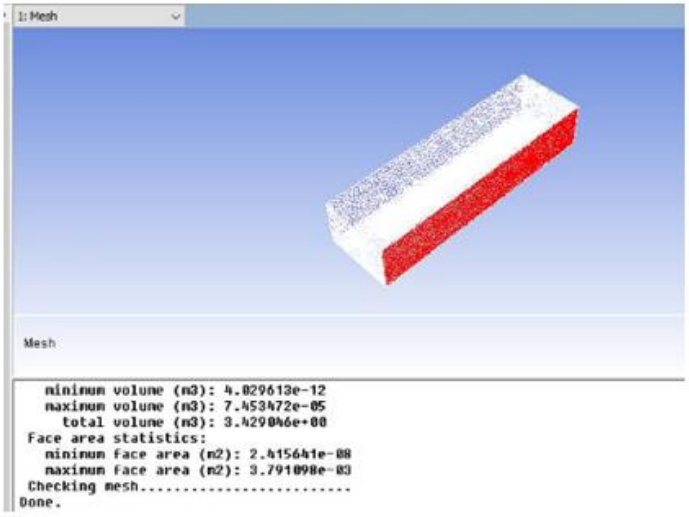

Figure 18: CFD Analysis

The computational results showed a maximum lift coefficient of 1.9604 and a major lift-to-drag ratio at 0°.

2.5 Construction

2.5.1 Materials

- Balsa Wood of 1/8x6x36
- Two spars of aluminum 2024
- LASERWOOD Baltic Birch Plywood 1/8x24x36
- Pro Adhesive 6-Min Epoxy

2.5.2 Tools

- Laser cutter
- Machine blade

2.5.3 Process

- A laser cutter was used to produce the 20 ribs required
- The machine blade was used to cut the two aluminum spars at the correspondent wing span size.
- Ribs were distributed along the spars, according to the location of the wing sections calculated on the lift distribution.

International Research Journal of Innovations in Engineering and Technology (IRJIET)

ISSN (online): 2581-3048

Volume 5, Issue 4, pp 87-96, April-2021

https://doi.org/10.47001/IRJIET/2021.504014

- Ribs and spars were joined with the Pro Adhesive.

III. RESULTS AND DISCUSSIONS

On Table V it is presented a brief summary of the results obtained on each stage of the design. Also, on Fig. 19 it is shown the flight circuit of the UAV using the fixed wing designed, lifting 22 kilograms of gross weight.

Table V: Results of the Aerodynamic Analysis

Wing Loading	**137.9** $\frac{N}{m^2}$
Wing Surface	1.7778 m^2
CL_{max_w}	1.7677
cl_{max_gross}	1.9641
Airfoil	E423
cl_{max}	2.0536
Reynolds Number	653,680.62
Wing Configuration	High double tapered wing
Aspect Ratio	7.9098
Taper Ratio	Half of the wing 1 and rest 0.6
Wing Span	3.75m
Root Chord	0.5267
Tip Chord	0.3160
Offset	12.6650
CL_{max} **obtained by the wind tunnel test**	1.9545
CL_{max} **obtained by the lift distribution**	2.005
CL_{max} **obtained with the methodology of Abbot**	1.8880
CL_{max} **obtained by CFD**	1.9604
Wing angle of stall	16°
Maximum lift-to-drag-ratio	19.78
Angle of incidence	0°

Figure 19: Flight Circuit

IV. CONCLUSIONS

The results of the methodology implemented on this research showed that the theoretical CL_{max_w}= 1.8880 had an approximation of 96.30% with the CFD outcome. However, the CL_{max_w}. ca1culated was 1.7677, which means that the wing theoretically generated 10.90% of extra lift. On the other hand, the experimental results from the wind tunnel test were approximated on a 99.69% with the CFD outcome, and therefore, the construction of the prototype was feasible. During the flight, it was observed that the fixed wing designed was capable to lift the 22 kilograms of gross weight of the UAV fulfilling the design requirements.

The implementation of a Systems Engineering (SE) management tool, such as, the System Life Cycle permitted to organize all the design tasks and test needed to achieve the design requirements. The methodology also allowed presenting the mathematical basis to design and model fixed wings capable of generating the force required to lift an UAV. All in all, the research accomplishes the objective to present a functional methodology to perform an aerodynamic analysis and develop a fixed wing model.

REFERNCES

[1] M. H. Sadraey, "Aircraft Design: A Systems Engineering Approach", *John Wiley & Sons, Ltd.*, 2013.

[2] Technical Commission, "Regular Class Official Contest Rulesl", *SAE Aero Design, México*, Revision NC, 2018.

[3] M. Simons, "Model Aircraft Aerodynamics", *Argus Books*, 1993.

[4] S. G. Kontogiannis, J. A. Ekaterinaris, "Design, performance evaluation and optimization of a UAV", *Aerospace Science and Technology*, 29, pp. 339-350, 2013.

[5] P. Raymer, "Aircraft Design: A Conceptual Approach", *American Institute of Aeronautics and Astronautics Inc.*, 1992.

[6] G. E. García, J. Nevárez, G. Fernández, X. Chávez, K. Olivares, "AerodynamicandControlAnalysis for anUnmannedAircraft", *IOS Press*, pp. 143-150, 2017.

[7] J. D. Anderson "Introduction to Flight", *McGraw-Hill Series in Aeronautical and Aerospace Engineering*, 1989.

[8] H. Abbott, A. E. Von Doenhoff, "Theory of wing sections, Including a Summary of Airfoil Data", *Dover Publications*, 1959.

[9] J. D. Anderson, "Aircraft Performance and Design", *WCB/McGraw-Hill*, 1999.

International Research Journal of Innovations in Engineering and Technology (IRJIET)

ISSN (online): 2581-3048

Volume 5, Issue 4, pp 87-96, April-2021

https://doi.org/10.47001/IRJIET/2021.504014

Citation of this Article:

Manuel Alejandro Lira Martinez, Arturo Paz Perez, Christian Aguirre Terrazas, Abril Abigail Solis Salazar, Julio Cesar Cuellar Mata, "Analysis of the Aerodynamics Parameters and Design of the Fixed Wing for the Drone" Published in *International Research Journal of Innovations in Engineering and Technology - IRJIET*, Volume 5, Issue 4, pp 87-96, April 2021. Article DOI https://doi.org/10.47001/IRJIET/2021.504014

****

